THE JOURNAL OF BIOLOGICAL CHEMISTRY VOL. 290, NO. 4, pp. 2251–2263, January 23, 2015

Differential Ubiquitin Binding by the Acidic Loops of Ube2g1 and Ube2r1 Enzymes Distinguishes Their Lys-48-ubiquitylation Activities*

Received for publication, November 17, 2014 Published, JBC Papers in Press, December 3, 2014, DOI 10.1074/jbc.M114.624809

Yun-Seok Choi[‡§¶1,2], Yun-Ju Lee[‡1], Seo-Yeon Lee[‡1], Lei Shi[‖], Jung-Hye Ha[‡§], Hae-Kap Cheong[‡], Chaejoon Cheong[‡§], Robert E. Cohen[¶], and Kyoung-Seok Ryu[‡§3]

From the [‡]Division of Magnetic Resonance, Korea Basic Science Institute Ochang Campus, Cheongwon-Gun, Ochang-Eup, Yangcheong-Ri 804-1, Chungcheongbuk-Do 363-883, [§]Department of Bio-Analytical Science, University of Science and Technology, Daejon 305-333, South Korea, [‖]Department of Bioengineering, University of Washington, Seattle, Washington 98195, and [¶]Department of Biochemistry and Molecular Biology, Colorado State University, Fort Collins, Colorado 80523-1870

Background: The acidic loops of E2 enzymes are important for their Lys-48-ubiquitylation activity.
Results: The presence of Tyr residues modulates the ubiquitin binding property of the acidic loop.
Conclusion: A proper interaction of the acidic loop with the attached donor ubiquitin is important for Lys-48-ubiquitylation activity.
Significance: One of molecular bases to study the mechanism of Lys-48-ubiquitylation is provided.

The ubiquitin E2 enzymes, Ube2g1 and Ube2r1, are able to synthesize Lys-48-linked polyubiquitins without an E3 ligase but how that is accomplished has been unclear. Although both E2s contain essential acidic loops, only Ube2r1 requires an additional C-terminal extension (184–196) for efficient Lys-48-ubiquitylation activity. The presence of Tyr-102 and Tyr-104 in the Ube2g1 acidic loop enhanced both ubiquitin binding and Lys-48-ubiquitylation and distinguished Ube2g1 from the otherwise similar truncated Ube2r1$^{1-183}$ (Ube2r1C). Replacement of Gln-105–Ser-106–Gly-107 in the acidic loop of Ube2r1C (Ube2r1C^{YGY}) by the corresponding residues from Ube2g1 (Tyr-102–Gly-103–Tyr-104) increased Lys-48-ubiquitylation activity and ubiquitin binding. Two E2∼UB thioester mimics (oxyester and disulfide) were prepared to characterize the ubiquitin binding activity of the acidic loop. The oxyester but not the disulfide derivative was found to be a functional equivalent of the E2∼UB thioester. The ubiquitin moiety of the Ube2r1C^{C93S}-[^{15}N]UB^{K48R} oxyester displayed two-state conformational exchange, whereas the Ube2r1C$^{C93S/YGY}$-[^{15}N]UB^{K48R} oxyester showed predominantly one state. Together with NMR studies that compared UB^{K48R} oxyesters of the wild-type and the acidic loop mutant (Y102G/Y104G) forms of Ube2g1, *in vitro* ubiquitylation assays with various mutation forms of the E2s revealed how the intramolecular interaction between the acidic loop and the attached donor ubiquitin regulates Lys-48-ubiquitylation activity.

The modification of proteins by ubiquitylation is important for the regulation of a large variety of cellular processes that includes cell cycle control, endocytosis, DNA repair, and regulation of transcription (1, 2). E3 ligases mediate the formation of isopeptide bonds between the C-terminal carboxyl group of ubiquitin and a Lys side chain of the target protein (monoubiquitylation) or a previously attached ubiquitin (polyubiquitylation). Although many kinds of ubiquitin-ubiquitin linkages are present *in vivo* (3), Lys-48-linked polyubiquitin chains, which direct ubiquitylated proteins to the 26 S proteasome complex for their degradation, are the most abundant ubiquitin signals. RING-E3 ligases are the dominant E3 species that mediate the direct transfer of ubiquitin (4) from the E2∼UB thioester intermediate to a target protein (2). An interaction between E2∼UB and ubiquitin is likely to be necessary for efficient Lys-48 polyubiquitylation, but such an interaction remains poorly characterized. In contrast, for Lys-63-linked ubiquitylation by the Ubc13 (E2) and Mms2 (ubiquitin-E2 variant) complex, Mms2 recruits an acceptor ubiquitin and positions its Lys-63 side chain in close proximity to the active site Cys of Ubc13 (5, 6). In a recent molecular docking model for Lys-11-ubiquitin linkage formation by Ube2S (7) based on NMR chemical shift perturbation (CSP)[4] data and *in vitro* ubiquitylation assay, Ube2S has binding surfaces for both acceptor and donor ubiquitin to position them and generate Lys-11-linkage polyubiquitin, whereas Ubc13 needs Mms2 to bind to and position an acceptor ubiquitin. In this model the interaction between donor ubiquitin or acceptor ubiquitin and Ube2S was very weak. Analogous mechanisms for the formation of Lys-48 ubiquitin linkages are unknown, possibly because interactions that guide Lys-48-ubiquitylation may be very weak and difficult to identify.

An *in vitro* E3-independent ubiquitylation assay that used p27-E2 fusion proteins had identified Ube2d2 (UbcH5b) and

* This work was supported, in whole or in part, by National Institutes of Health Grant GM097452 (to R. E. C.). This study was also supported by the high-field NMR research program from Korea Basic Science Institute (KBSI; to K.-S. R.) and KBSI Grant T33410 (to H.-K. C.).
[1] These authors contributed equally to this work.
[2] Supported by University of Science and Technology Post-Doc research program.
[3] To whom correspondence should be addressed. Tel.: 82-43-240-5064; Fax: 82-43-240-5059; E-mail: ksryu@kbsi.re.kr.

[4] The abbreviations used are: CSP, chemical shift perturbation; HSQC, heteronuclear single quantum coherence; TROSY, transverse relaxation optimized spectroscopy; UB, ubiquitin; Ube2r1C, Ube2r1 (1–183); Ube2r1C^{YGY}, Ube2r1C (Q105Y/S106G/G107Y); HSQC, heteronuclear single quantum correlation.

Ube2b (hHR6b) as the most efficient mediators for the ubiquitylation of p27, but those E2s were found to be less effective for subsequent Lys-48-ubiquitylation in comparison to Ube2r1 (human Cdc34) (8). Recent reports showed that the sequential engagement of two different E2 enzymes may be important for efficient polyubiquitylation of target proteins in an E3-dependent system. UbcH5 was found to be efficient for the first ubiquitylation of IκBα, but then Ube2r1 performed the subsequent Lys-48-ubiquitylation reactions in the presence of Skip/Cullin/F-box E3 complex (9). Ube2r1 is able to synthesize Lys-48-linked polyubiquitin chains efficiently without an E3 ligase. This E3-independent reaction mechanism is likely to be used as well by the E2 during the RING-E3-mediated ubiquitylation.

Both Ube2g1 (human Ubc7) and Ube2r1 possess an acidic loop in the vicinity of the active-site Cys residue and display an exceptional ability to synthesize Lys-48-linked polyubiquitin chains. The acidic loops contain several Asp and Glu residues, and mutations eliminating these negative charges have been shown to decrease the ubiquitylation activity of yeast Cdc34 in the presence of the Skip/Cullin/F-box E3 complex (10). Ube2k, which lacks the acidic loop, has a similar ability for Lys-48-specific polyubiquitylation, whereas most other E2 enzymes cannot synthesize Lys-48 polyubiquitin efficiently in the absence of an E3 ligase (11). Ube2g1 consists of only an E2-core domain, but Ube2r1 has an additional C-terminal extension (residues 184–236). Work from our group previously showed that, unlike full-length Ube2r1, the Ube2r1 core (residues 1–183; Ube2r1C) has a decreased capability to synthesize Lys-48 polyubiquitin chains efficiently in the absence of an E3 (8). Ube2d2, which does not have an acidic loop, also is unable to synthesize Lys-48 polyubiquitin in the absence of an E3 ligase (8) despite having ubiquitin binding affinity almost identical to that of Ube2g1 as assessed by NMR CSP experiments using [^{15}N]UB (12).

In this study we focused on the acidic loops and ubiquitin binding activities of Ube2g1 and Ube2r1C. By comparing ubiquitin binding and polyubiquitin synthesis by Ube2g1, Ube2r1C, and Ube2d2, their different abilities to synthesize Lys-48-linked chains were evaluated with respect to intramolecular interaction between the acidic loop and the attached donor ubiquitin.

EXPERIMENTAL PROCEDURES

Protein Preparations—Genes encoding E2 enzymes (*ube2g1*, *ube2r1*, and *ube2d2*) and ubiquitin variants (His- or non-tagged) were cloned into the pGEX-4T-1 (BamHI/XhoI) and pET15b/pET21a (NdeI/XhoI) vectors, respectively. Point mutations were introduced using the QuikChange site-directed mutagenesis kit (Stratagene). All proteins were expressed in the *Escherichia coli* strains BL21 DE3 or Rosetta DE3. The proteins were purified using GSTrap and HisTrap chromatography columns (GE Healthcare), respectively. The attached GST or His tags were cleaved by thrombin digestion followed by thrombin inactivation with 1 mM PMSF and benzamidine-HCl. Target proteins were further purified by gel permeation chromatography using Superdex-75 (GE Healthcare); where applicable, subsequent passage through a GSTrap column was used to remove the cleaved GST. Murine E1 protein was purified following a previously reported method (8), and the concentration of the E1 stock solution (~2.0 mg/ml) was estimated based on band intensity observed after sodium dodecyl sulfate polyacrylamide gel electrophoresis (SDS-PAGE) and staining with Coomassie Blue.

All of the isotope-enriched proteins for NMR experiments were obtained by growing *E. coli* in M9 minimal medium supplemented with [^{15}N]NH_4Cl (0.1%) and [^{13}C]glucose (0.2%). The (i) random fractional (75~80%) and (ii) complete (~97%) deuteration of proteins were done by growing *E. coli* in M9 minimal medium (99% D_2O) supplemented with (i) [^{13}C]glucose (0.2%) and [^{15}N]NH_4Cl (0.1%) or (ii) [^{13}C,^{2}H]glucose (0.2%), ^{13}C,^{2}H,^{15}N-labeled Celton powder (0.1%, Cambridge Isotope Laboratory), and [^{15}N]NH_4Cl (0.1%), respectively (13, 14).

In Vitro Ubiquitylation Assay—*In vitro* ubiquitylation was done using 200~300 μM ubiquitin, 20 μM E2, and ~0.5 μM E1 in a reaction buffer (pH 7.0, 7.5, or 8.0) composed of 50 mM Tris-HCl, 1 mM DTT, 2 mM ATP, 2 mM $MgCl_2$, 10 mM creatine phosphate, and 1 unit each of pyrophosphatase and creatine phosphokinase at 25 °C. The reaction products were separated by 14~16% SDS-PAGE. The formation of E2~UB thioester was evaluated by non-reducing SDS-PAGE in which the reaction mixtures were sampled 20 min after the addition of E1 and then quickly frozen in liquid nitrogen.

To estimate the approximate K_m values for E2-mediated Lys-48-ubiquitylation, the *in vitro* ubiquitylation assays were performed with 1.5 μM E1 and increasing ubiquitin concentrations from 0.2 to 2.4 mM. The amounts of diubiquitin synthesized were estimated by integrating the diubiquitin bands in the Coomassie Blue-stained SDS-PAGE gel using the Multi Gauge program (Fujifilm). The reaction sample containing the highest concentration of the ubiquitin substrate was serially diluted and separated in the same SDS-PAGE as an internal reference to confirm the linearity of the integrated band intensities. Sample loadings were reduced to ensure that the volume integrals of diubiquitin bands correlated linearly to the amounts loaded; two or more experimental replicates were done for each E2 enzyme. The establishment of a stable concentration of E2~ubiquitin thioester was associated with a time lag during which the product was not synthesized constantly. Therefore, the amount of synthesized di-UB is lower than expected, and this error was high at low concentrations of substrate ubiquitin. Nevertheless, the volume integrals of the diubiquitin bands were fitted with the Michaelis-Menten equation to estimate relative K_m values of different E2s.

Preparation of E2-UB Oxyester and E2-UB Disulfide Derivatives—E2-UB oxyesters were synthesized using the active-site Cys-to-Ser mutant E2 protein (Ube2g1^{C90S} or Ube2r1C^{C93S}) in reactions with a UB^{K48R}:E2 molar ratio of 2. Instead of wild-type UB, intact or His_6-tagged UB^{K48R} was used here to prevent loss of E2-UB oxyesters caused by Lys-48 diubiquitin formation and to facilitate product purification. The amounts of E1 used were up to 10× larger than was used in the standard ubiquitylation assay; more E1 was required for Ube2g1^{C90S} than for Ube2r1C^{C93S} due to the higher hydrolysis rate of Ube2g1^{C90S}-UB^{K48R} oxyester. The ubiquitin-coupling reactions were done in a buffer (pH 8.0) consisting of 50 mM Tris·HCl, 1 mM DTT, 4 mM ATP, 5 mM $MgCl_2$, 20 mM creatine phosphate, and 2 units of pyrophosphatase and creatine phosphokinase. The reaction

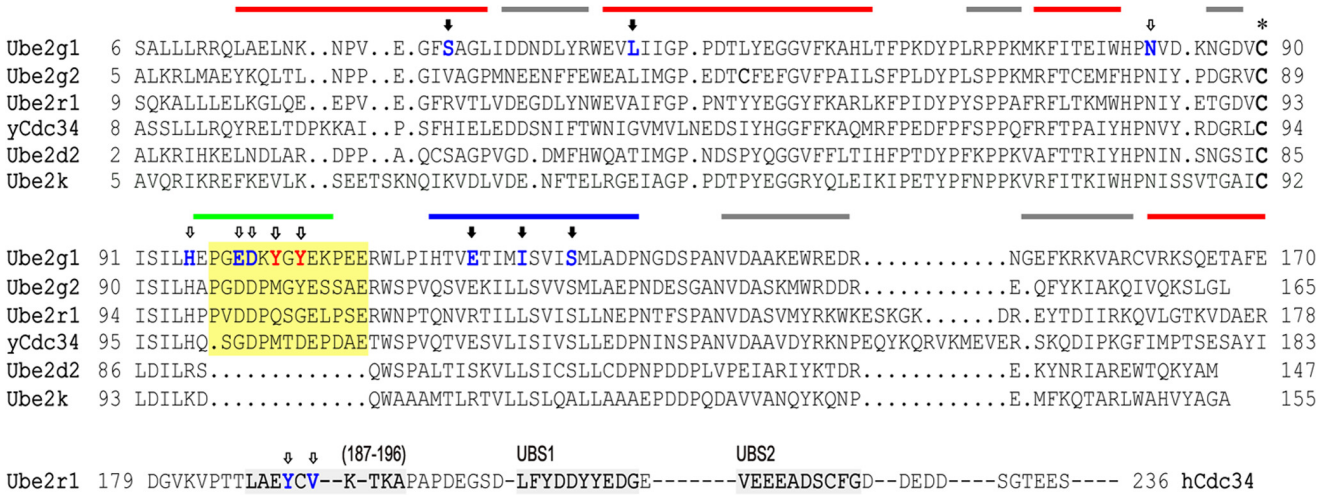

FIGURE 1. **Structure-based sequence alignment of E2 enzymes.** The sequence alignment was performed through structural matching of the E2 enzymes using the Chimera program (24). The previously identified non-covalent ubiquitin-binding sites of the Ube2r1 C-terminal tail (26) are marked with a *gray highlight*, and the acidic loop region is indicated by a *yellow highlight*. The *asterisk* represents the active-site Cys residues of the E2 enzymes. Ube2g1 and Ube2r1 residues that when mutated resulted in a decrease in Lys-48-ubiquitylation activity are indicated by *open arrows*, and those that have no activity change are indicated by *closed arrows*. The surface of Ube2g1 is roughly divided into four areas for better description of the data; the bottom side (*red bar*), the acidic loop (*green bar*), the left side (*blue bar*), and the right side (*gray bar*).

temperature and time were 35~37 °C and 6 h for Ube2g1^{C90S} and 30~33 °C and 15 h for Ube2r1C^{C93S}.

The synthesized [^{15}N]Ube2g1^{C90S}-UB^{K48R} oxyesters were separated from the remaining Ube2g1^{C90S} by His-tag affinity column chromatography, and the remaining free His-tagged UB^{K48R} was completely removed by gel permeation chromatography using Superdex-75 column in a buffer (pH 7.0) containing 50 mM HEPES and 100 mM NaCl. To minimize hydrolysis during purification, the products (*i.e.* Ube2g1^{C90S}-[^{15}N]UB^{K48R} or Ube2r1C^{C93S}-[^{15}N]UB^{K48R} oxyester) were purified only by gel permeation chromatography; as a result, those purified E2-UB oxyester proteins contained 20~30% of the free E2 proteins.

Disulfide-linked complexes of Ube2r1C and [^{15}N]UB$^{K48R/G76C}$, generated essentially by following the previously reported protocol (15), were made in which N-terminal His-tagged [^{15}N]UB$^{K48R/G76C}$ was attached to Ube2r1 via a disulfide bond. The E2-UB disulfide complex was purified by His-tag affinity column chromatography followed by gel permeation chromatography after thrombin-catalyzed removal of the His tag.

NMR Experiments and Backbone Chemical Shift Assignments—NMR spectra were recorded using the 800- and 900-MHz (cryogenic probe) Bruker spectrometers in the Korea Basic Science Institute at 25 °C. NMR samples were prepared in a buffer (pH 7.0) containing 50 mM HEPES, 100 mM NaCl, and 10% D_2O; 1~2 mM DTT was included, except in the case of E2-UB disulfide complexes. NMR data were processed using the NMRPipe program (16) and analyzed using the SPARKY program (17). K_d values were obtained from titrations by fitting CSP data to a simple binding equation in which the CSP values were measured as $[\Delta N^2 + (6\times\Delta H)^2]^{1/2}$ (12).

TROSY triple-resonance experiments were used for the backbone chemical shift assignment of [^{13}C,^{2}H,^{15}N]Ube2g1, and resonance assignments of [^{13}C,^{15}N]Ube2g1 and [^{13}C,^{15}N]Ube2g1$^{Y102G/Y104G}$ were determined by comparing their HSQC and three-dimensional-HNCA spectra with those of [^{13}C,^{2}H,^{15}N]Ube2g1. The HSQC peaks of [^{13}C,^{15}N]Ube2d2 were assigned by using the previously reported chemical shifts (4).

Rosetta Docking Model of Ube2g1^{C90S}-UB^{K48R} Based on the NMR CSP Data—Homology-based model structures of Ube2g1 were generated from the SWISS-MODEL server (18) and CS-Rosetta (19) using the assigned chemical shifts of Ube2g1; the two model structures generated in this way were almost identical (root mean square deviation 0.97 Å). The C90S mutation was generated from the CS-Rosetta model of Ube2g1. We first performed rigid-body docking between the attached donor UB^{K48R} and Ube2g1^{C90S} with Patchdock (20) using the chemical shift perturbation data from both UB^{K48R} and Ube2g1^{C90S} as constraints. The acidic loop (residues Glu-96—Trp-111) was removed during the rigid-body docking step. Starting from the Patchdock rigid models with the incomplete acidic loop, we used the RosettaCM program (21) to build the acidic loop and simultaneously refine the rigid body orientations between UB^{K48R} and Ube2g1^{C90S}. The backbone atoms of both proteins in the complex model were allowed to move with constraint to initial backbone during the flexible refinement, and 2000 refined models are generated. The final ensemble structures were selected by their clustering and interface scores. The overall CSP of Ube2g1^{C90S}-UB^{K48R} oxyester matched well to the previously reported docking models of Ubc1~UB thioester (22) and Cdc34~UB thioester (23). All molecular visualizations were done using the Chimera program (24).

RESULTS

Despite Their Similar Domain Structures, the Lys-48 Polyubiquitylation Activity of Ube2r1C Is Much Lower Than That of Ube2g1—Sequence alignment of several E2 enzymes (Ube2g1, Ube2g2, Ube2r1, yeast Cdc34, Ube2d2, and Ube2k) shows that Ubc7 homologs (Ube2g1 and Ube2g2) and Cdc34 homologs (Ube2r1 and yeast Cdc34) have a distinct 12- or 13-residue insertion sequence in the vicinity of the active-site Cys (Fig. 1); this sequence was designated as an acidic loop due to the pres-

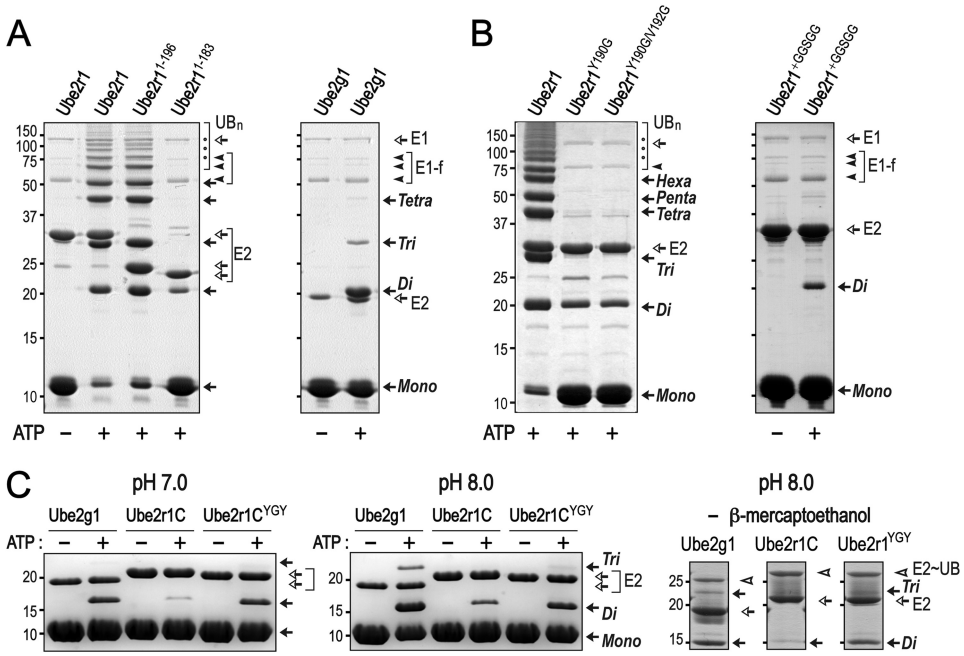

FIGURE 2. **E3-independent Lys-48 ubiquitylation activities of Ube2g1, Ube2r1, and Ube2r1 mutants.** The *in vitro* ubiquitylation reactions were performed using E1 (~0.5 μM), E2 (20 μM), and ubiquitin (0.2 mM) in a buffer containing 50 mM Tris-HCl (pH 7.5). Ubiquitin and the polyubiquitin products are marked *Mono*, *Di*, *Tri*, etc. *A*, Ube2r1 requires C-terminal residues 184–196 for wild-type activity. The activity of Ube2r1$^{1-183}$ (Ube2r1C) was much lower than that of either Ube2r1 or Ube2g1. *B*, the Ube2r1 mutant proteins (Y190G and Y190G/V192G) showed significant impairment in their *in vitro* ubiquitylation activities. The insertion of a GGSGG sequence between Val-183 and Pro-184 of Ube2r1 resulted in a complete loss of Lys-48 ubiquitylation activity. *C*, Ube2r1C^{YGY} had Gln-105–Ser-106–Gly-107 in the acidic loop replaced by the Tyr-102–Gly-103–Tyr-104 sequence from Ube2g1. Although the Lys-48-ubiquitylation activity of Ube2r1C was lower than that of Ube2g1, Ube2r1C^{YGY} showed activity to a level close to that of Ube2g1 (*left panel*). The formation of E2~UB thioester adducts by Ube2g1, Ube2r1C, and Ube2r1C^{YGY} was assessed by non-reducing SDS-PAGE analysis. Samples were prepared in SDS-PAGE loading buffer without β-mercaptoethanol 15 min after the ubiquitylation reaction was initiated with ATP. The three enzymes showed similar amounts of E2~UB thioester intermediate formation (*right panel*).

ence of many negatively charged Asp and Glu residues in yeast Cdc34 (10) (Fig. 1). Both Ube2g1 and Ube2r1 can synthesize Lys-48-linked polyubiquitin adducts in the absence of E3 ligase. However, despite the close similarity of their sequences (52% identity and 68% similarity), the *in vitro* ubiquitylation activity of Ube2r1 core enzyme (Ube2r1C, residues 1–183) was much lower than that of Ub2g1; Ube2r1 required a C-terminal extension (at a minimum, residues 184–196) for efficient Lys-48-ubiquitylation (Fig. 2*A*). Mutations within residues 184–196 of Ube2r1 (*i.e.* Y190G or Y190G/V192G) significantly impaired Lys-48-ubiquitylation activity, and the insertion of a GGSGG spacer between Val-183 and Pro-184 of Ube2r1 also greatly decreased the ubiquitylation activity (Fig. 2*B*).

Ubiquitylation assays in which the E2 concentration was varied showed that the length of Lys-48 polyubiquitin products increased with increasing the concentration of Ube2r1 (Fig. 3). This result is consistent with the previous report that the dimerization of Ube2r1 increases its Lys-48-ubiquitylation activity (25). On the other hand, with Ube2g1 the size distribution of Lys-48 polyubiquitin products did not depend on the E2 concentration, and thus catalysis by Ube2g1 likely involves a reaction between the E2~UB thioester and an acceptor ubiquitin that is not associated with a second E2~UB molecule. In comparison with Ube2r1, the relatively simple ubiquitylation reaction by Ube2g1 suggested that studies focused on Ube2g1 and comparisons with Ube2d2 and Ube2r1C might reveal a mechanistic relationship between the ubiquitin binding activity and Lys-48-ubiquitylation.

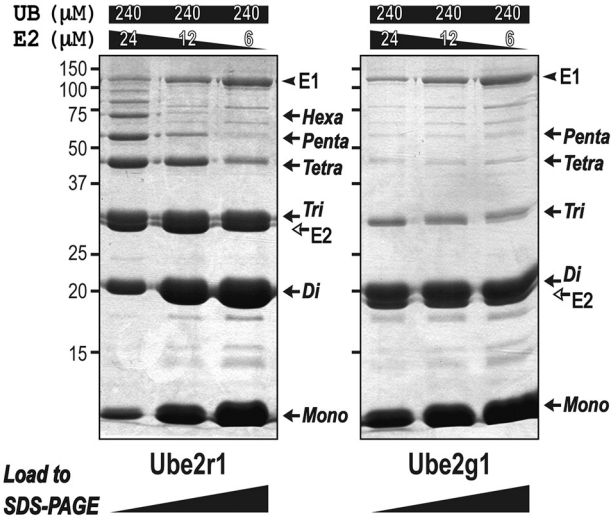

FIGURE 3. **The E2 concentration dependence of *in vitro* ubiquitylation by Ube2r1 and Ube2g1.** The amount of E1 needed to produce maximal Lys-48-ubiquitylation activity was first determined to ensure that the activation of E2 by E1 was not rate-limiting. The synthesis of Lys-48-linked triubiquitin and higher polyubiquitin by Ube2r1 was dependent on the E2 concentration. This result is consistent with a previous report that the dimerization of Ube2r1 increases its Lys-48-ubiquitylation activity. However, the concentration dependence of Ube2g1 indicated that catalysis by Ube2g1 likely involves a reaction between E2-UB thioester and a free acceptor ubiquitin.

Two Aromatic Residues (Tyr-102 and Tyr-104) in the Ube2g1 Acidic Loop Are Important for Non-covalent Ubiquitin Binding—Previous NMR CSP experiments using [^{15}N]UB showed that the ubiquitin binding properties of Ube2d2 are similar to those of

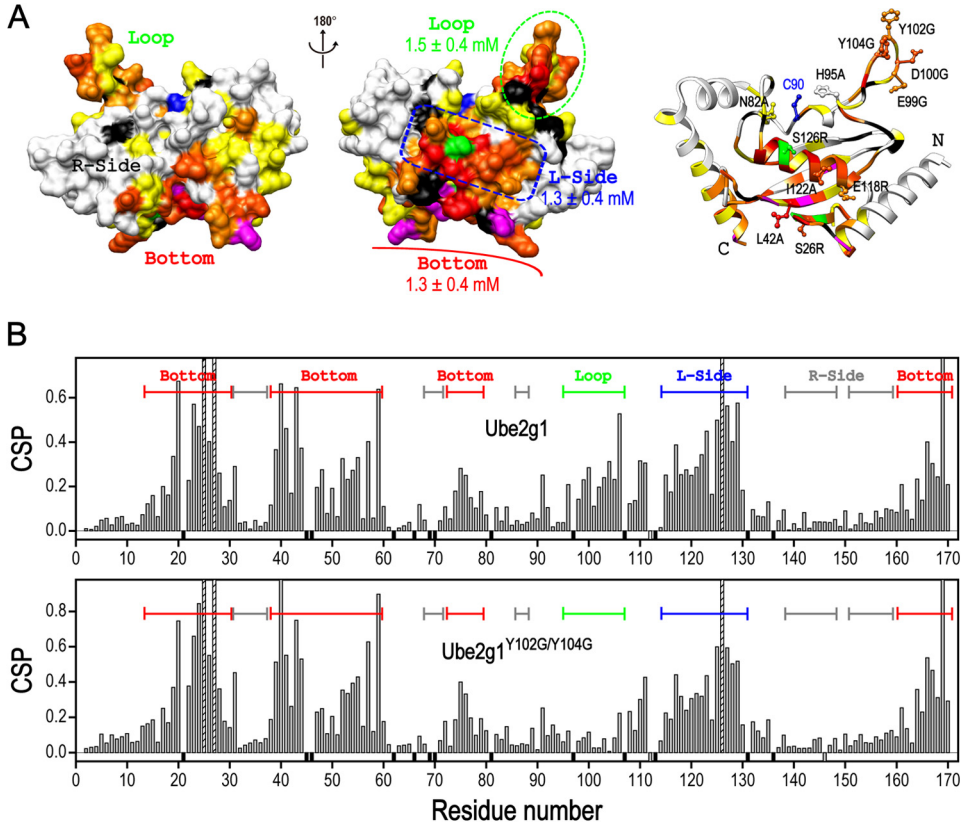

FIGURE 4. **Comparison of the non-covalent ubiquitin-binding surfaces of Ube2g1 and Ube2g1$^{Y102G/Y104G}$.** *A*, ubiquitin binding surfaces of Ube2g1 as determined by CSP experiments in the presence of 0.5 mM ubiquitin. The *magenta*, *red*, *orange*, and *yellow* colors, respectively, indicate high to low magnitude of CSP. The peaks of Phe-25, Ala-27, and Ser-126 disappeared upon the addition of 0.5 mM ubiquitin and are in *green*. Residues in *black* represent prolines, which are not visible in the HSQC spectrum due to the absence of an amide proton. The original peak intensity of Leru-112 was too weak to determine the CSP and is, therefore, also in *black*. The ubiquitin binding surface of Ube2g1 can be separated into three parts, namely the bottom, L-side, and loop. The non-covalent ubiquitin binding affinities (K_d values) were measured by titrations with ubiquitin to be 1.25 ± 0.39, 1.32 ± 0.40, and 1.46 ± 0.36 mM for the bottom, L-side, and loop regions, respectively. *B*, the CSP data for [^{15}N]Ube2g1 and [^{15}N]Ube2g1$^{Y102G/Y104G}$ in the presence of 0.5 mM ubiquitin are represented as a *histogram*. The *striped bars* represent residues for which the resonance peaks disappeared in the presence of 0.5 mM ubiquitin. The *negative black* and *gray bars* represent, respectively, Pro residues or residues where peak intensities were too weak to be detected in the CSP experiment. Note that Ube2g1$^{Y102G/Y104G}$ lost ubiquitin interactions only in the acidic loop region.

Ube2g1 (12), although Ube2d2 lacks an acidic loop and also cannot synthesize Lys-48 polyubiquitin chains efficiently in the absence of an E3 (8). We now have compared the ubiquitin-interacting surfaces of Ube2g1 and Ube2d2 in detail. Interestingly, CSP signals from the acidic loop region of Ube2g1 (*Loop*) were clearly identified when ubiquitin was added (Fig. 4, *A* and *B*, *top panel*). Two other major non-covalent ubiquitin binding surfaces of Ube2g1 (*bottom* and *L-side*) are very similar to those in Ube2d2 (data not shown). The presence of three ubiquitin binding surfaces in Ube2g1 (K_d = 1.25 ± 0.39, 1.32 ± 0.40, and 1.46 ± 0.36 mM for bottom, L-side, and loop regions, respectively) can explain the lower apparent K_d value (0.56 ± 0.17 mM) that was previously determined from the CSP experiments using [^{15}N]UB and Ube2g1 (12). The acidic loop in Ube2g1 is similar to the previously characterized weak ubiquitin-binding site 1 (UBS1) in the C-terminal tail of Ube2r1 (DLFYDDYYED) (26), which also consists of hydrophobic and acidic residues (Fig. 1). The T1, T2, and ^{1}H,^{15}N heteronuclear NOE values measured for Ube2g1 showed that the acidic loop region is more flexible than the bulk of the structured E2 core (data not shown); this finding is consistent with recent NMR ^{15}N relaxation data for Ube2g2 (27).

Sequence alignment of Ube2g1 and Ube2r1C revealed two critical differences in their acidic loop regions: Tyr-102 and Tyr-104 in Ube2g1 correspond to Gln-105 and Gly-107 in Ube2r1 (Fig. 1). To assess the effect of Tyr-102 and Tyr-104 on non-covalent ubiquitin binding by Ube2g1, both were mutated to Gly residues (Ube2g1$^{Y102G/Y104G}$). After the assignment of the backbone chemical shifts of [^{13}C,^{15}N]Ube2g1$^{Y102G/Y104G}$, CSPs were measured upon titration with unlabeled ubiquitin. Although the ubiquitin binding properties of the bottom and L-side regions of the mutant of Ube2g1 were unchanged, the CSPs from the loop region completely disappeared (Fig. 4*B*). Thus, the two Tyr residues are critical for non-covalent ubiquitin binding of the acidic loop in Ube2g1.

Introduction of Two Tyr Residues into the Ube2r1C Acidic Loop Increased Both Ubiquitin Binding Affinity and Lys-48-ubiquitylation Activity—We changed Gln-105–Ser-106–Gly-107 in Ube2r1C to Tyr-105–Gly-106–Tyr-107 (Ube2r1C^{YGY}) to make its acidic loop more similar to that of Ube2g1 and then assessed the *in vitro* ubiquitylation activity. The introduction of two Tyr residues into the Ube2r1C acidic loop greatly increased Lys-48-ubiquitylation activity to a level close to that of Ube2g1 (Fig. 2*C*). Non-reducing SDS-PAGE showed that the activity dif-

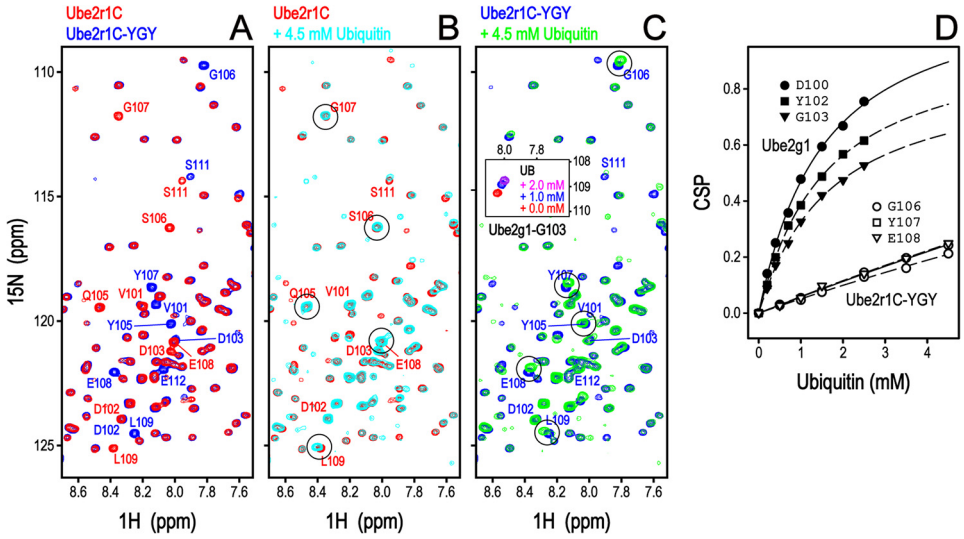

FIGURE 5. **HSQC perturbation experiment of [^{15}N]Ube2r1C and [^{15}N]Ube2r1C^{YGY} in the presence of ubiquitin.** *A*, substitution of the Gln-105–Ser-106–Gly-107 residues in the Ube2r1C acidic loop by the Tyr-102–Gly-103–Tyr-104 sequence from Ube2g1 changed the chemical shifts of several residues. The HSQC peaks that originated from the flexible acidic loop (residues 101–112) and the N- and C-terminal regions (residues 1–6 and 182–183) were assigned by using the ^{13}C,^{15}N-labeled protein. Although the chemical shifts of the region, including the Gln-105–Ser-106–Gly-107 residues of Ube2r1C, were mostly unchanged even in the presence of 4 mM ubiquitin (*B*), the region changed to Tyr-105–Gly-106–Tyr-107 was clearly perturbed by the addition of ubiquitin (*C*). The HSQC spectrum of the region representing the Gly-103 residue of [^{15}N]Ube2g1 in the presence of 0.0, 1.0, and 2.0 mM ubiquitin are shown for the reference of CSP amount (*inset*). *D*, [^{15}N]Ube2g1 or [^{15}N]Ube2r1C^{YGY} is titrated by ubiquitin, and the titration curves of the selected residues are plotted.

ferences between wild-type Ube2r1C and Ube2r1C^{YGY} were not the result of impaired E2~UB thioester formation (Fig. 2*C*, *right panel*).

It has been reported that the C-terminal extension of Ube2r1 includes two weak ubiquitin binding motifs (UBS1, residues 205–214, and UBS2, residues 216–225) and an additional possibility of a third, very weak ubiquitin-binding site (residues 187–196) (26). However, Ube2r1C alone did not detectably bind to [^{15}N]UB (data not shown); the low background with Ube2r1C made identification of ubiquitin binding differences between Ube2r1C and Ube2r1C^{YGY} straightforward. Comparison of the HSQC spectra between Ube2r1C and Ube2r1C^{YGY} showed that the effect of Tyr-105–Gly-106–Tyr-107 substitution was limited to the backbone chemical shifts only of the acidic loop residues (Fig. 5*A*). The CSP data showed that the acidic loop of Ube2r1C^{YGY}, but not Ube2r1C, had a non-covalent interaction with ubiquitin (Fig. 5). However, the CSP magnitudes of the [^{15}N]Ube2r1C^{YGY} acidic loop were very small even in the presence of 4.5 mM ubiquitin, and thus the exact affinity for ubiquitin could not be determined. This low ubiquitin binding affinity together with the high Lys-48-ubiquitylation activity of Ube2r1C^{YGY} compared with Ube2r1C suggested a possible role for the acidic loop in an intramolecular interaction with E2 thioester-linked donor ubiquitin.

Synthesis of E2-UB Oxyester for NMR Experiments—To characterize the intramolecular interaction between the acidic loop and the E2-attached donor ubiquitin used for Lys-48-ubiquitylation, we tried to obtain more stable E2-UB complexes as oxyester adducts. Crystal structures of the Ube2d2-UB oxyester alone (28) and its complex with a HECT-family E3 ligase (29) have been reported, and NMR studies on Ube2d3 (UbcH5c)-UB and Ubc13-UB oxyesters have been described (30). Interestingly, using a high concentration of E1, the ubiquitin-charging reaction with Ube2g1^{C90S} at 35 °C produced not only the Ube2g1^{C90S}-UB oxyester but also appreciable amounts of Lys-48-linked diubiquitin. In comparison, the same reaction using Ube2r1C^{C93S} required less E1 and mostly produced the Ube2r1C^{C93S}-UB oxyester and only a small amount of diubiquitin (Fig. 6*A*). These results are evidence that the E2-UB oxyester is a functional mimic of the labile E2~UB thioester. The ubiquitin K48R mutant (UB^{K48R}) was used to prepare the [^{15}N]Ube2g1^{C90S}-UB^{K48R} oxyester on a large scale, but spontaneous hydrolysis of the E2-UB oxyester was detected during the purification even at 4 °C (Fig. 6*B*). We monitored the spontaneous hydrolysis at 25 °C of the Ube2g1^{C90S}-UB^{K48R} and Ube2r1C^{C93S}-UB^{K48R} oxyesters by SDS-PAGE analysis and found that the Ube2r1C^{C93S}-UB^{K48R} oxyester ($t_{1/2}$ ~ 20 h) was more stable than the Ube2g1^{C90S}-UB^{K48R} oxyester ($t_{1/2}$ ~ 5 h) (Table 1).

The Donor Ubiquitin of Ube2r1C^{C93S}-[^{15}N]UB^{K48R} Oxyester Exhibited Two-state Conformational Exchange, Whereas the Ubiquitin in the Ube2r1C$^{C93S/YGY}$-UB^{K48R} Oxyester Preferred One Conformation—Unfortunately, the very complex HSQC spectrum of the [^{15}N]Ube2r1C^{C93S}-UB^{K48R} oxyester made detailed characterization by NMR difficult. The peak intensities of the HSQC spectra overall were very weak and inhomogeneous (data not shown). For more clear analyses by NMR of the oxyester adducts, we reduced the number of HSQC peaks by preparation of the Ube2r1C^{C93S}-[^{15}N]UB^{K48R} and Ube2r1C$^{C93S/YGY}$-[^{15}N]UB^{K48R} oxyesters. We also prepared chemically stable Ube2r1C-[^{15}N]UB$^{K48R/G76C}$ and Ube2r1C^{YGY}-[^{15}N]UB$^{K48R/G76C}$ disulfide adducts, as Ube2r1C contains only one Cys residue (*i.e.* Cys-93 at the active site). Interestingly, the HSQC spectra of disulfide-linked Ube2r1C-[^{15}N]UB$^{K48R/G76C}$ were greatly different from those of the Ube2r1C^{C93S}-[^{15}N]UB^{K48R} oxyester (Fig. 7). The HSQC peaks from [^{15}N]UB^{K48R} in the oxyesters were much less intense than those from the disulfide-linked [^{15}N]UB$^{K48R/G76C}$ due to motion (*i.e.* conformational exchange) in an intermediate-to-slow NMR

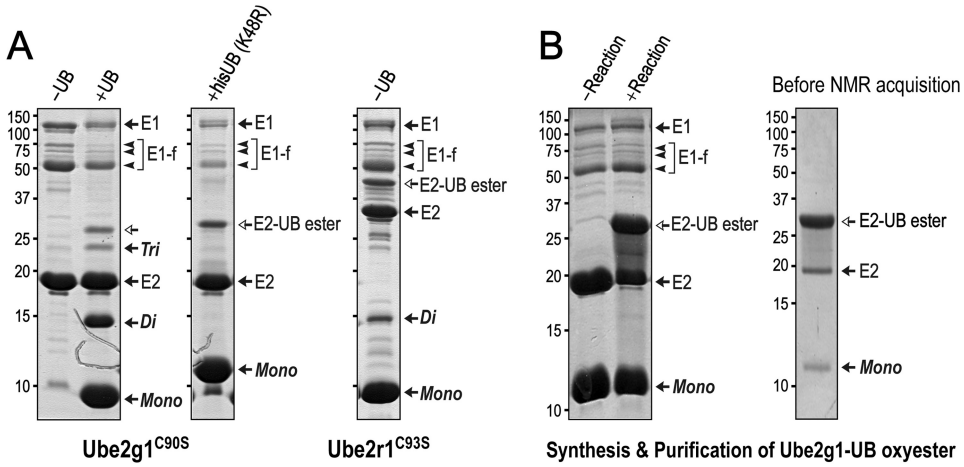

FIGURE 6. **Synthesis and purification of the Ube2g1^{C90S}-UB^{K48R} oxyester.** *A*, the *in vitro* ubiquitylation of Ube2g1^{C90S} with ~2.0 μM E1 at 35 °C and pH 8.0 produced not only the Ube2g1^{C90S}-UB oxyester but also appreciable amounts of diubiquitin (*Di*). The Ube2g1^{C90S}-UB^{K48R} oxyester was synthesized with His-tagged UB^{K48R} instead of wild-type UB. The same reaction using Ube2r1^{C93S} mostly produced the Ube2r1^{C93S}-UB oxyester intermediate, and a small amount of diubiquitin product also was detected. *B*, a longer incubation with concentrations of ~2.0 μM E1, 200 μM E2, and 400 μM UB^{K48R} produced a large amount of the Ube2g1^{C90S}-UB^{K48R} oxyester (*left panel*). His-tagged UB^{K48R} was used to facilitate purification of the E2-UB oxyester product. However, the stability of the E2-UB oxyester was relatively low, and its spontaneous hydrolysis was apparent during the purification even at 4 °C (*right panel*).

TABLE 1

Spontaneous hydrolysis rates of various E2-UB oxyesters at 25 °C

E2-UB^{K48R} oxyester	Half-life
	h
Ube2g1^{C90S}-[^{15}N]UB^{K48R}	8.8 ± 1.1[a]
Ube2g1$^{C90S/Y102G/Y104G}$-[^{15}N]UB^{K48R}	5.8 ± 0.2[a]
Ube2g1^{C90S}-UB^{K48R}	6.4 ± 1.7[b]
Ube2g1$^{C90S/Y102G/Y104G}$-UB^{K48R}	2.8 ± 0.4[b]
Ube2r1^{C93S}-UB^{K48R}	24.3 ± 5.9[b]
Ube2r1$^{C93S/YGY}$-UB^{K48R}	20.0 ± 6.5[b]

[a] The donor ubiquitin was 13C/2H/15N-labeled; the hydrolysis rates (shown here as $t_{1/2}$) in buffer (pH 7.0, 50 mM HEPES and 100 mM NaCl) were determined from the several well separated HSQC peaks.

[b] The hydrolysis rates (i.e., $t_{1/2}$ values) at pH 8.0 were determined from two or more separate measurements using non-reducing SDS-PAGE analysis.

time scale that caused severe broadening and disappearance of the peaks. The ubiquitin CSPs of the oxyester relative to the chemical shifts of free [^{15}N]UB^{K48R} and also the CSPs of the disulfide adducts relative to free [^{15}N]UB$^{K48R/G76C}$ showed that the [^{15}N]UB^{K48R} moiety of the oxyester had much larger CSPs than with the disulfide-linked [^{15}N]UB$^{K48R/G76C}$ (Fig. 8, *A* and *B*). Many peaks of the Ube2r1C^{C93S}-[^{15}N]UB^{K48R} oxyester were split into two sets; these corresponded to the major hydrophobic surface patch that includes residue Ile-44 of ubiquitin. However, with the Ube2r1C$^{C93S/YGY}$-[^{15}N]UB^{K48R} oxyester, these resonances were not split and remained as one set (Fig. 7*A*). This effect was much smaller or absent with the disulfide adducts where possible splittings in only a few peaks were barely identified for the Ube2r1C-[^{15}N]UB$^{K48R/G76C}$ disulfide but not for the Ube2r1C^{YGY}-[^{15}N]UB$^{K48R/G76C}$ disulfide (Fig. 7*B*). Overall, evidence of intramolecular interaction between the donor ubiquitin and Ube2r1C was greatly reduced with the disulfide adduct relative to the oxyester adduct. A possible explanation is that, compared with the E2-UB oxyester linkage, the E2-UB disulfide is a poorer mimic of the physiological thioester (*e.g.* it is longer by approximately one S atom) and may interfere with the normal intramolecular interaction between the acidic loop and the donor ubiquitin.

The HSQC spectra indicated that the ubiquitin in the Ube2r1C^{C93S}-[^{15}N]UB^{K48R} oxyester has two different conformations but that one conformation is preferred in the YGY-mutant complex (*i.e.* the Ube2r1C$^{C93S/YGY}$-[^{15}N]UB^{K48R} oxyester). The major set of peaks in the HSQC spectrum of the Ube2r1C^{C93S}-[^{15}N]UB^{K48R} oxyester displayed much larger CSPs than did the minor set, whereas the Ube2r1C$^{C93S/YGY}$-[^{15}N]UB^{K48R} oxyester displayed one set of peaks whose CSP magnitudes were similar to those of the minor set in the HSQC spectrum of the Ube2r1C^{C93S}-[^{15}N]UB^{K48R} oxyester (Fig. 8*A*). The absence of apparent non-covalent UB binding activity in Ube2r1C can explain why the donor ubiquitin exhibits (at least) two different conformations in its Ube2r1C^{C93S}-[^{15}N]UB^{K48R} oxyester form. Both weak intermolecular interactions can be entropically stabilized in an intramolecular association. The intensified interactions of the donor ubiquitin with both the L-side and the acidic loop of Ube2r1C, by competing with each other, can produce two sets of HSQC peaks. The introduction of the two Tyr residues into the acidic loop of Ube2r1C likely shifts the equilibrium by stabilizing the interaction between the donor UB and the acidic loop. However, we cannot exclude a possibility that the preferred conformation is caused by other mechanisms, such as a conformational change accompanying binding. The chemical shift differences between Ube2r1C^{C93S}-[^{15}N]UB^{K48R} and Ube2r1C$^{C93S/YGY}$-[^{15}N]UB^{K48R} oxyesters showed that the interaction between the E2 and the hydrophobic patch of the donor ubiquitin was reduced more for Ube2r1C$^{C93S/YGY}$ than for Ube2r1C^{C93S} (Fig. 8*A*).

Proposed Role of the Ube2g1 Acidic Loop for the Efficient Lys-48-ubiquitylation in the Absence of E3—We prepared Ube2g1-UB oxyesters to obtain more detailed information about the intramolecular interaction between Ube2g1 and the donor ubiquitin. Interestingly, the HSQC spectrum of the [^{15}N]Ube2g1^{C90S}-UB^{K48R} oxyester was well dispersed (Fig. 9*A*). Previous reports have shown that the [^{15}N]Ube2d3~UB thioester mostly lost discernible HSQC peaks due to intermolecular interaction mediated by the attached donor ubiquitin and another [^{15}N]Ube2d3~UB (31). The donor ubiquitin of the Ube2d3$^{C85S/S22R}$-[^{15}N]UB oxyester has been found in an

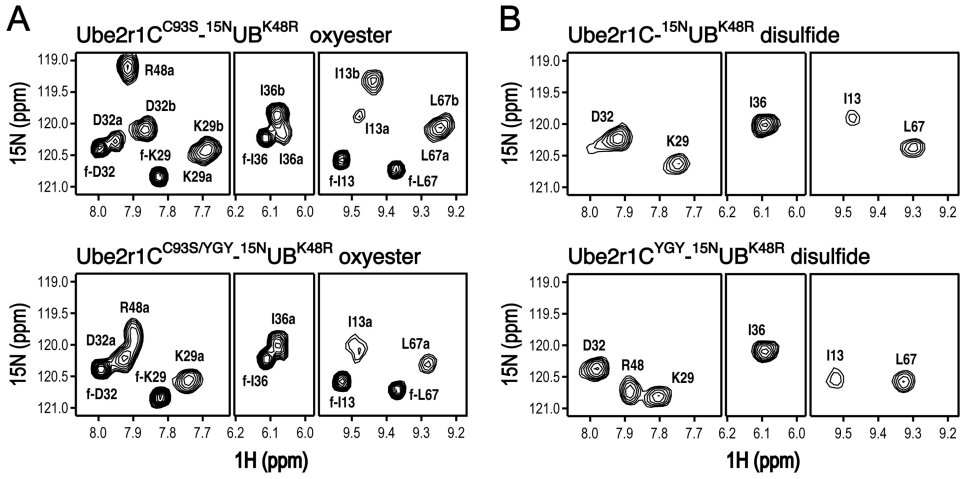

FIGURE 7. **HSQC spectra of Ube2r1C^{C93S}- and Ube2r1C$^{C93S/YGY}$-[^{15}N]UB^{K48R} oxyesters (*A*) and Ube2r1C- and Ube2r1C^{YGY}-[^{15}N]UB^{G76C} disulfides (*B*).** *A*, selected regions of the HSQC spectra show that the attached donor ubiquitin of the Ube2r1C^{C93S}-[^{15}N]UB^{K48R} oxyester has two different conformations (*top panel*) but that of the Ube2r1C$^{C93S/YGY}$-[^{15}N]UB^{K48R} oxyester has one predominant conformation (*bottom panel*). Residues labeled with an *f-* are residues from ubiquitin that had dissociated from the E2. *B*, the same regions of the HSQC spectra of disulfide-linked Ube2r1C-[^{15}N]UB$^{K48R/G76C}$ and Ube2r1C^{YGY}-[^{15}N]UB$^{K48R/G76C}$ show that in both complexes the attached donor ubiquitin mostly has a single conformation and that the chemical shift differences from free ubiquitin are much smaller than with the oxyester complexes.

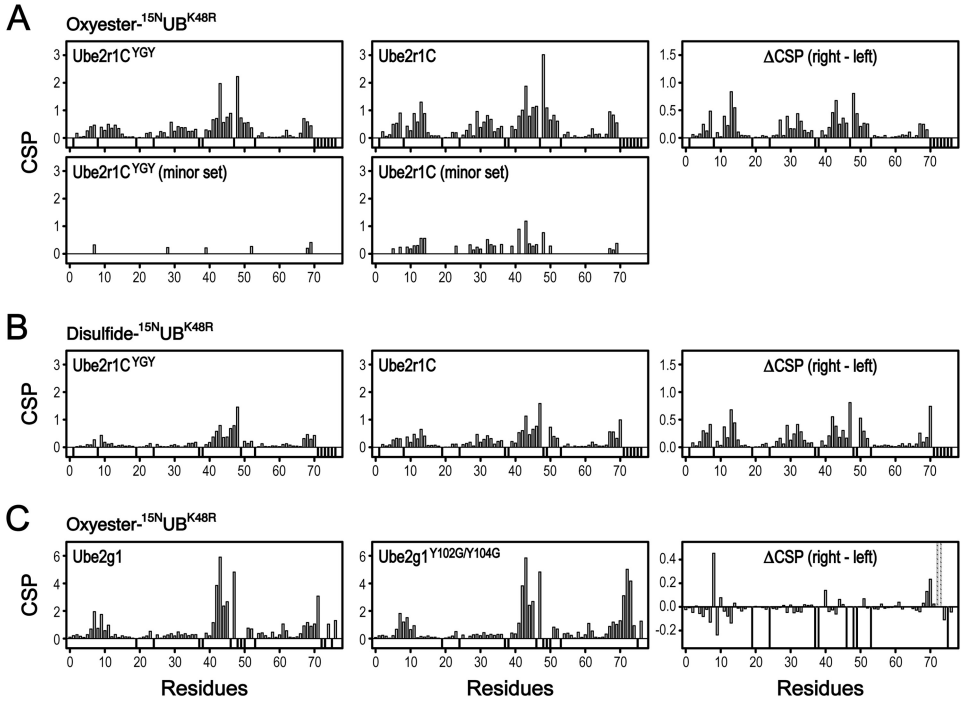

FIGURE 8. **Chemical shift perturbations relative to free [^{15}N]UB of [^{15}N]UB resonances in the Ube2r1C$^{C93S/YGY}$-[^{15}N]UB^{K48R} and Ube2r1C^{C93S}-[^{15}N]UB^{K48R} oxyesters (*A*), Ube2r1C^{YGY}-[^{15}N]UB$^{K48R/G76C}$ and Ube2r1C-[^{15}N]UB$^{K48R/G76C}$ disulfides (*B*), and Ube2g1^{C90S}-[^{15}N]UB^{K48R} and Ube2g1$^{C90S/Y102G/Y104G}$-[^{15}N]UB^{K48R} oxyesters (*C*).** The chemical shifts of free [^{15}N]UB^{K48R} and [^{15}N]UB$^{K48R/G76C}$ were used to determine the CSPs of E2-[^{15}N]UB^{K48R} oxyesters and disulfides, respectively. The chemical shift differences between the attached [^{15}N]UB molecules of the wild-type and the acidic-loop mutant E2 are shown in the *right panels*. The *negative bars* represent the residues including prolines (Pro-19, Pro-37, and Pro-38) for which peaks were not shown in the HSQC spectra. The *dotted bars* in *C* (*right panel*) represent the residues apparent in the HSQC spectra of the Ube2g1^{C90S}-[^{15}N]UB^{K48R} oxyester but not the Ube2g1$^{C90S/Y102G/Y104G}$-[^{15}N]UB^{K48R} oxyester.

extended and dynamic state, referred to as an "open conformation," that is not favorable for its ubiquitylation activity (30). Ube2g1 has UB binding surfaces similar to Ube2d3; in Ube2d3~UB, these promote the self-association of Ube2d3~UB. However, because there was no disappearance or significant decrease of HSQC peaks of the UB-oxyester when compared with [^{15}N]Ube2g1, the [^{15}N]Ube2g1^{C90S}-UB oxyester apparently lacks the intermolecular interaction.

Although we could not fully assign the HSQC peaks of the [^{15}N]Ube2g1^{C90S}-UB^{K48R} oxyester, comparisons of the HSQC and three-dimensional-HNCO spectra between [^{15}N]Ube2g1^{C90S}-UB^{K48R} oxyester and free [^{15}N]Ube2g1^{C90S} made it possible to determine the interaction surface on Ube2g1 for the attached donor ubiquitin (Fig. 9). The HSQC peaks of the acidic loop and many other residues, especially those on the L-side, were changed too much to be traced reli-

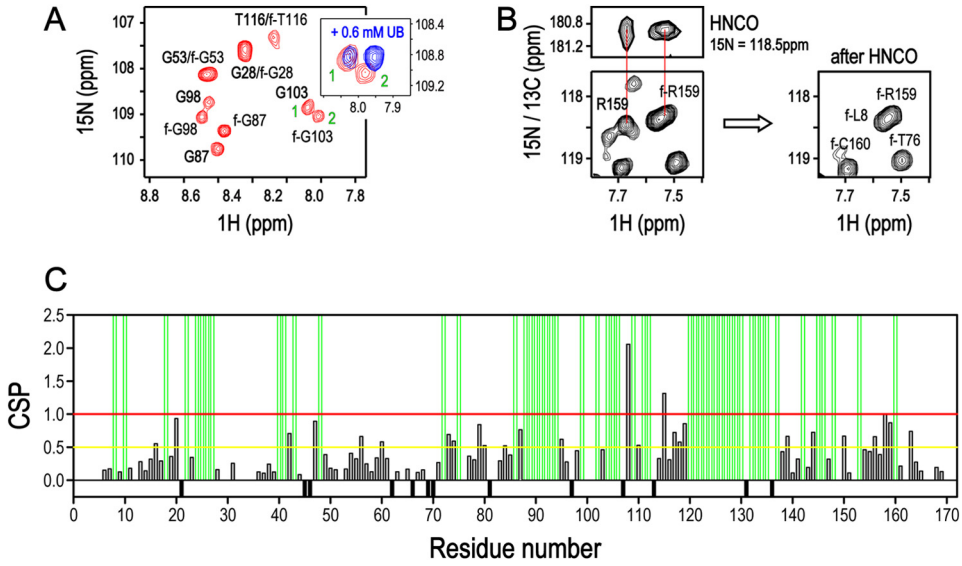

FIGURE 9. **Assignment of HSQC spectrum of [^{15}N]Ube2g1^{C90S}-UB^{K48R} oxyester.** *A*, two sets of ^{1}H,^{15}N HSQC peaks were identified resulting from the [^{15}N]Ube2g1-UB^{K48R} oxyester and free [^{15}N]Ube2g1 (labeled with *f-*), respectively. Nevertheless, the well dispersed spectrum of the purified [^{15}N]Ube2g1^{C90S}-UB^{K48R} oxyester shows the absence of an intermolecular interaction between the attached donor ubiquitin and different Ube2g1 molecules. *Inset*, interestingly, the peak from the Gly-103 residue of the [^{15}N]Ube2g1-UB^{K48R} oxyester was not strongly perturbed by additional free ubiquitin (0.6 mM) compared with that of free [^{15}N]Ube2g1, suggesting that the Gly-103 residues were affected differently by added (*i.e.* acceptor) ubiquitin in the presence of the oxyester-attached donor ubiquitin. *B*, the HSQC-peaks assignment of [^{15}N]Ube2g1^{C90S}-UB^{K48R} oxyester was performed by comparing the HSQC spectra with [^{15}N]Ube2g1^{C90S}-UB^{K48R} oxyester and with [^{15}N]Ube2g1^{C90S} hydrolyzed from its oxyester adduct. The residues displaying very similar peak positions in the HSQC spectrum for the oxyester and free form were assigned unambiguously, and some of additional residues were also assigned based on the HNCO spectrum. *C*, the CSPs of [^{15}N]Ube2g1^{C90S} between the oxyester and free form are shown as a *bar plot*. The residues for which chemical shifts were too different between the oxyester and free form to be clearly assigned are indicated using *green bars*.

ably from the spectrum of free [^{15}N]Ube2g1^{C90S} to the [^{15}N]Ube2g1^{C90S}-UB^{K48R} oxyester (Figs. 9*C* and 10*A*). This result contrasts with Ube2d3$^{C85S/S22R}$-[^{15}N]UB oxyester (30) in which the chemical shift differences between the oxyester-bound and free [^{15}N]UB were relatively small. To determine in more detail the binding mode of the donor ubiquitin in the Ube2g1-UB oxyester, we also prepared oxyester complexes of Ube2g1^{C90S} and Ube2g1$^{C90S/Y102G/Y104G}$ using [^{13}C,^{2}H,^{15}N]UB^{K48R}. Due to their low stability in solution and larger chemical shift changes compared with TROSY peaks of free [^{13}C,^{2}H,^{15}N]UB^{K48R}, the ^{1}H,^{15}N TROSY peaks of Ube2g1^{C90S}-[^{13}C,^{2}H,^{15}N]UB^{K48R} were assigned using additional TROSY-based three-dimensional-HNCO spectra. From time-dependent changes in the TROSY spectra, we also determined the half-lives of [^{15}N]Ube2g1^{C90S}- and [^{15}N]Ube2g1$^{C90S/Y102G/Y104G}$-[^{2}H,^{15}N]UB^{K48R} oxyesters to be 8.8 ± 1.1 and 5.8 ± 0.2 h, respectively (Table 1). The comparison of TROSY peaks from free and attached [^{13}C,^{2}H,^{15}N]UB^{K48R} showed that the hydrophobic patch of the attached donor ubiquitin interacts with the L-side of Ube2g1 (Fig. 8*C*).

The CSP-based Rosetta docking model of the acidic loop-deleted Ube2g1^{C90S}-UB^{K48R} oxyester together with additional fitting of the loop based on CSPs provided structural insight about the intramolecular interaction between the E2 acidic loop and the attached donor ubiquitin (Fig. 10). Although the exact modeling of the acidic loop structure in the Ube2g1^{C90S}-UB^{K48R} oxyester was difficult, the geometric constraint of the oxyester bond shows that the YGY segment of the acidic loop is likely to be located in the vicinity of Arg-74 of the donor ubiquitin. The active site of the Ube2g1^{C90S}-UB^{K48R} oxyester appears to be accessible only through the R-side of Ube2g1 because the L-side was completely occupied by the attached donor ubiquitin (Fig. 10*E*). Our data clearly supported the idea that an acceptor ubiquitin approaches the R-side of Ube2g1; this result agrees well with the recently reported docking model of Ube2S~UB thioester in which L-side positioning of the donor ubiquitin is important for the activity of Lys-11 ubiquitin-linkage formation (7). The chemical shift differences of [^{15}N]UB^{K48R} molecules between Ube2g1^{C90S}-[^{15}N]UB^{K48R} and Ube2g1$^{C90S/Y102G/Y104G}$-[^{15}N]UB^{K48R} oxyesters were much smaller than those between the free and attached [^{15}N]UB^{K48R}. The acidic loop mutation (Y102G/Y104G) changed the chemical shifts of specific residues of donor [^{15}N]UB^{K48R} that were localized along one edge of the hydrophobic patch extending to the C terminus (Fig. 8*C* and Fig. 10*C*). Therefore, the intramolecular interaction between the donor ubiquitin and the L-side of Ube2g1 seemed overall to be identical for both Ube2g1^{C90S} and Ube2g1$^{C90S/Y102G/Y104G}$. Thus, the complex structure (Fig. 10*C*) caused by the intramolecular interaction between the donor ubiquitin and the L-side of Ube2g1 or Ube2g1$^{Y102G/Y104G}$ is not the only requirement for Ube2g1 ubiquitylation activity. Our model for the Ube2g1-UB oxyester suggests that the interaction of the acidic loop with the donor ubiquitin helps to stabilize binding of the acceptor ubiquitin. The interaction surface for the acceptor ubiquitin is located on the R-side and is composed of the C-terminal region of the donor ubiquitin, the region of the acidic loop that includes residues Glu-99 and Glu-100, and additional Ube2g1 residues near Cys-90 at the active site.

To estimate the K_m values for ubiquitin in E3-independent ubiquitylation reactions by Ube2g1, Ube2g1^{Y104G}, and Ube2r1C^{YGY}, we measured the steady-state rates of diubiquitin formation as a function of ubiquitin concentration (Fig. 11).

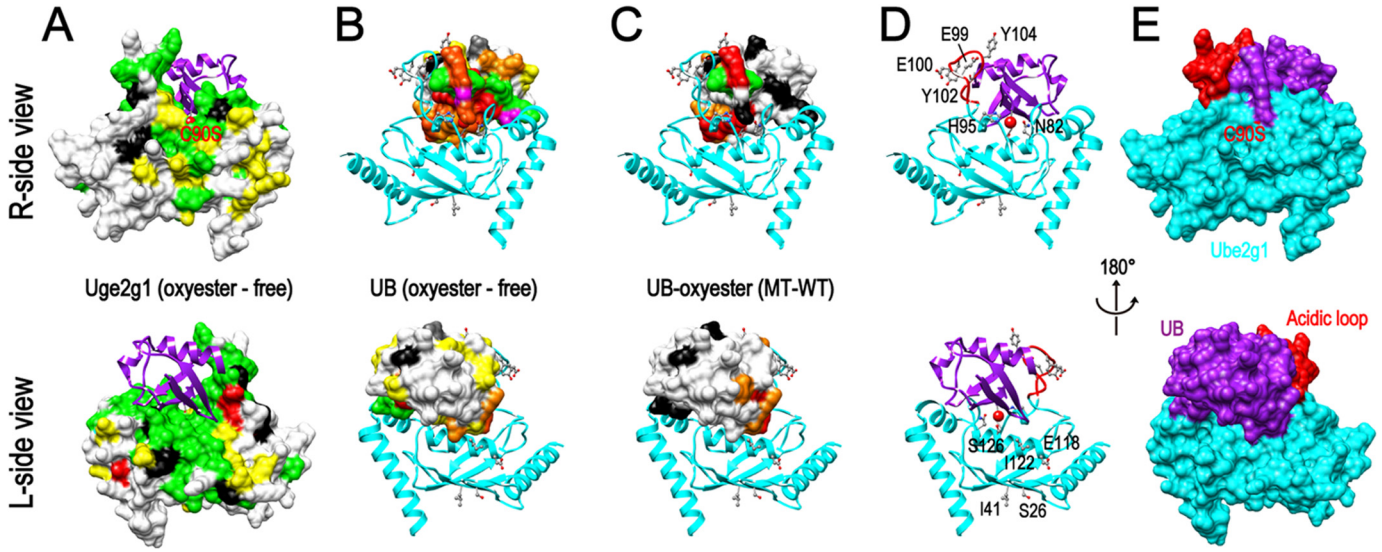

FIGURE 10. **The interaction surfaces between UB^{K48R} and Ube2g1^{C90S} mapped on a model of the oxyester complex.** *A*, intramolecular UB^{K48R}-interaction surfaces on Ube2g1^{C90S} are highlighted on the structure of free Ube2g1. The *red* and *yellow colors*, respectively, indicate high and low magnitude CSPs. The residues in which the HSQC peaks shifted too much to be traced are shown in *green* (see Fig. 9*C*). *B*, Ube2g1^{C90S}-interacting surface of UB^{K48R} is highlighted using *magenta*, *red*, *orange*, and *yellow* colors to indicate high to low magnitude of CSPs, respectively. The residues colored *black* represent prolines and other residues that were invisible in the HSQC spectrum, and the *green*-colored residues indicate where resonances disappeared in the oxyester complex. *C*, the residues of UB^{K48R} showing different chemical shifts between the oxyesters with Ube2g1^{C90S} and Ube2g1$^{C90S/Y102G/Y104G}$ are highlighted as in *panel B*. *D*, the residues of Ube2g1 mutated for the ubiquitylation assays (Fig. 12) are shown superimposed onto a ribbon representation of the structure. *E*, surface presentation shows the donor UB^{K48R}-occupied surface of the E2.

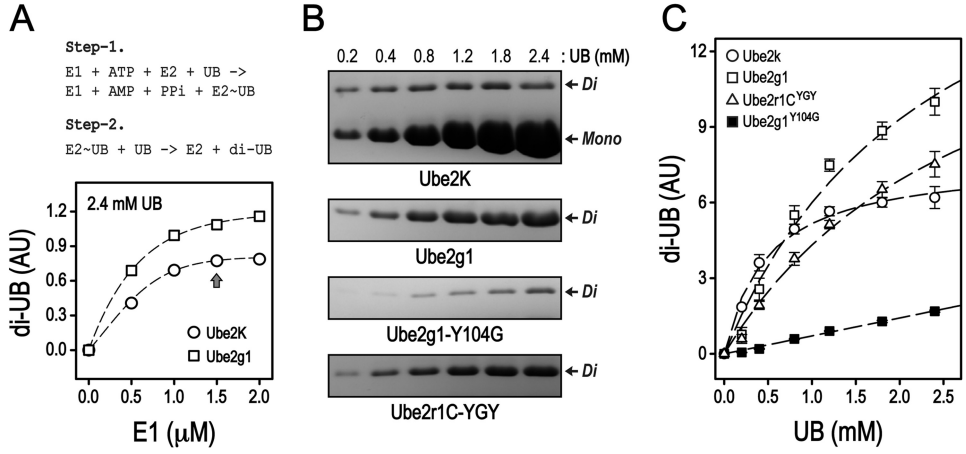

FIGURE 11. ***In vitro* ubiquitylation by Ube2k, Ube2g1, Ube2g1^{Y104G}, or Ube2r1C^{YGY} in the presence of various concentrations of ubiquitin.** *A*, the reaction of di-UB synthesis can be divided into two steps (I and *Step-2*). If the step-1 is faster than the step-2, the concentration of E2~UB is essentially constant (dt[E2~UB]/$dt \cong 0$). The ubiquitylation activity of Ube2k and Ube2g1 was assessed at pH 7.5 in the presence of increasing concentrations of E1 and with 2.4 mM ubiquitin. The E1 concentration used was ~1.5 μM for further steady-state kinetic analysis of E3-independent ubiquitylation. *AU*, absorbance units. *B*, the *in vitro* ubiquitylation reactions were performed in the presence of increasing concentration of the substrate ubiquitin with fixed concentrations of E1 and E2. The amount of the diubiquitin product bands increased as the concentration of the substrate ubiquitin increased. *C*, the K_m values of E2-mediated ubiquitylation were estimated for Ube2k, Ube2g1, Ube2g1^{Y104G}, and Ube2r1C^{YGY} from the modified Michaelis-Menten equation (see "Experimental Procedures"). The K_m value of Ube2K, Ube2g1, or Ube2r1^{YGY} was 0.5 ± 0.06, 2.5 ± 0.7, or 2.9 ± 0.7 mM, respectively. The K_m value of Ube2g1^{Y104G} was too high to be determined by this experiment.

The K_m and k_{cat} values for E3-independent ubiquitylation by Ube2k were reported previously to be 0.58 mM and 0.56 min^{-1}, respectively (11); thus, ubiquitylation by Ube2k was used as a reference to validate our steady-state kinetic analysis. The K_m value (~0.5 mM) we determined for Ube2k agreed well with the reported value. Although we could not determine exact K_m values due to a practical upper limit of several millimolar for the ubiquitin substrate in our assays, it was apparent that the K_m for Ube2g1^{Y104G} is at least severalfold greater than that of the wild-type Ube2g1 (Fig. 11). The K_m data suggest that Tyr-104 in the acidic loop is important for the interaction of Ube2g1~UB thioester with an acceptor ubiquitin. Importantly, the HSQC peak of Gly-103 in the [^{15}N]Ube2g1^{C90S}-UB^{K48R} oxyester form was shifted much less by the addition of free ubiquitin than that in [^{15}N]Ube2g1 alone (Fig. 9*A*, *inset*), which suggests that the intermolecular interaction between the acidic loop and an acceptor ubiquitin in the context of the Ube2g1-UB oxyester is different from that with free Ube2g1.

Mutation in the Acidic Loop Region Changed the in Vitro Ubiquitylation Activity of Ube2g1—We introduced various point mutations into each ubiquitin-interaction site (bottom, S26R and L41A; L-side, E118R, I122A, and S126R; loop, Y104G,

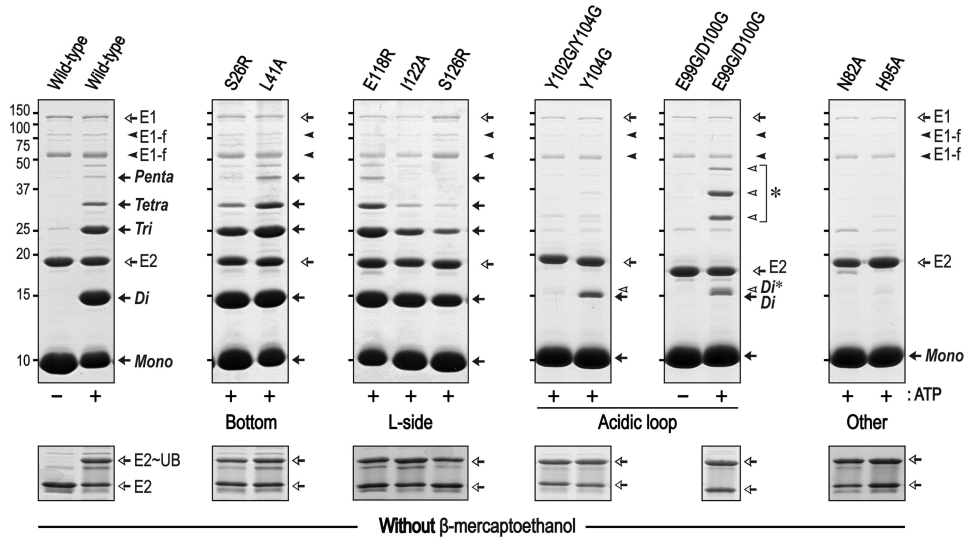

FIGURE 12. ***In vitro* ubiquitylation activities of Ube2g1 mutants in the absence of E3 ligase.** The *in vitro* ubiquitylation reaction was performed using E1 (~0.5 μM), E2 (20 μM), and ubiquitin (0.3 mM) in a 50 mM Tris-HCl (pH 7.5) buffer. Ubiquitin and ubiquitin oligomers are marked *Mono, Di, Tri*, etc. Ube2g1 mutants were generated in any of three independent non-covalent ubiquitin binding regions (S26R and L41A for the *bottom*; E118R, I122A, and S126R for the L-side; Y104G, Y102G/Y104G, E99G/D100G for the acidic loop) or two residues potentially involved directly in catalysis (N82A and H95A). Only the mutations in the ubiquitin binding region of the acidic loop and in the potential catalytic residues displayed a severe defect in E3-independent ubiquitylation. An additional diubiquitin band (*Di**) was identified for the Ube2g1 mutants that had decreased activity. Note that, although the apparent molecular size of the Ube2g1$^{E99G/D100G}$ determined by SDS-PAGE analysis was slightly lower than that of other Ube2g1 proteins, the correct molecular mass of 18,526 Da was confirmed by MALDI-TOF mass spectrometry. The reaction with Ube2g1$^{E99G/D100G}$ produced unidentified high molecular sized bands (marked with an *asterisk*) that probably reflect auto-ubiquitylation of the E2. The formation of Ube2g1~UB thioesters was assessed by non-reducing SDS-PAGE analysis (*bottom*). *AU*, absorbance units.

Y102G/Y104G, and E99G/D100G) to explore their effects on the ubiquitylation activity. Our rationale for choosing these mutations is as follows. Mutations in specific Ube2g1 residues (S26R and L41A in the bottom; E118R in the L-side) were determined from the sequence alignment with Ube2r1 (Fig. 1), because Ube2r1C did not display any detectable non-covalent ubiquitin binding. Ser-26 corresponds to Ser-22 of Ube2d3 (UbcH5c), and Ube2d3^{S22R} greatly decreases the ubiquitin binding activity (31). The I122A mutation corresponds to the L125A mutation of Ube2S; it was reported that Leu-125 is important for Lys-11-ubiquitylation activity by positioning the donor ubiquitin into the L-side of Ube2S (7). The results in Fig. 12 show that only the mutations in the acidic loop resulted in severe loss of Lys-48-ubiquitylation activity; none of the mutations in the bottom or L-side of Ube2g1 had significant defects in the ubiquitylation activity. The lower ubiquitylation activity did not result from an impaired formation of E2~UB thioester by E1 enzyme (Fig. 12, *bottom panel*). We additionally confirmed that the time-course activations of Ube2g1, Ube2g1^{S126R}, and Ube2g1^{Y104G} by E1 enzyme were almost identical, and their productions of diubiquitin species were gradually increased as increasing the incubation time from 0 to 2 h (data not shown).

The activity of the Y104G mutant was lower than that of the wild type, and the Y102G/Y104G mutant was nearly inactive. Other acidic loop mutations in Ube2g1 (*i.e.* E99G/D100G) also abolished ubiquitylation activity, which is in agreement with a previous report that showed decreased activity in the acidic loop mutants of yeast Cdc34 in the presence of Skip/Cullin/F-box-E3 (10). Residues Glu-99 and Asp-100 are located in the R-side of Ube2g1 (Fig. 10*D*). Interestingly, the ubiquitylation reaction catalyzed by Ube2g1$^{E99G/D100G}$ produced additional unidentified protein bands (shown by an *asterisk* in Fig. 12); these most likely reflect autoubiquitylation of the E2 itself.

Recent NMR studies of Ube2g2 proposed that His-94, which is positioned close to Cys-89 in the active site, is likely to have a catalytic role (27). His-94 corresponds to His-95 of Ube2g1 and is also conserved in Ube2r1 (Fig. 1). We confirmed that this His residue, like the Asn-82 residue that is evolutionarily conserved among E2 proteins and is important for the formation of a ubiquitin-protein linkage (32), is important for Lys-48-ubiquitylation activity. Either H95A or N82A mutants of Ube2g1 completely eliminated the ubiquitylation activity (Fig. 12). Other Ube2g1 His-95 mutants (H95R and H95E) similarly failed to show detectable activity (data not shown).

DISCUSSION

We have shown that the intramolecular interaction between the acidic loop of Ube2g1 and the donor ubiquitin plays an important role in the Lys-48-ubiquitylation activity of E2 enzymes. Ubiquitin binding properties of the acidic loop were investigated with two E2~UB thioester mimics, E2-UB oxyesters, and disulfides, and then the inferences regarding E2 Lys-48-ubiquitylation activity were confirmed by enzymatic assays using various point mutants. The Ube2g1-UB oxyester can serve as a functional analog of the labile E2~UB thioester intermediate. Ube2g1^{C90S} and Ube2r1C$^{C93S/YGY}$ were able to produce Lys-48 diubiquitin.

The presence of the cognate RING-E3 ligase restricts the dynamics of the donor ubiquitin in the Ube2d3-UB oxyester to a position (closed conformation) that is more favorable for the ubiquitylation reaction (33). Moreover, donor ubiquitins on Ube2S (7), Ubc1 (the yeast homolog of Ube2k) (22), and Ube2r1

(23) have been proposed to adopt closed conformations predicted to facilitate ubiquitylation. We have shown here that the donor ubiquitin in the Ube2g1-UB oxyester interacts with the L-side of Ube2g1 and thus adopts a closed conformation that is similar to the models suggested for Ube2S, Ubc1, and Ube2r1. However, adoption of the closed conformation by the donor ubiquitin through its interaction with the L-side of E2 does not seem to be critical for Lys-48-ubiquitylation by Ube2g1. The donor ubiquitin in Ube2g1$^{C90S/Y102G/Y104G}$-UB^{K48R} oxyester also can adopt the closed conformation, although no ubiquitylation activity was observed for the Ube2g1$^{Y102G/Y104G}$ mutant. Moreover, the introduction of two Tyr residues into the acidic loop of Ube2r1C stabilized a conformation of the donor ubiquitin that, according to NMR CSP data, reflected a decreased interaction between the hydrophobic patch of the donor ubiquitin and the L-side of Ube2r1C^{YGY} (Fig. 8*A*). Although both Ube2g1^{C90S} and Ube2r1C$^{C93S/YGY}$ displayed appreciable Lys-48-ubiquitylation activity, the configurations of their donor ubiquitin in the oxyester forms appeared to differ. Smaller CSPs (relative to free [^{15}N]UB^{K48R}) with the Ube2r1C$^{C93S/YGY}$-[^{15}N]UB^{K48R} oxyester than with the Ube2g1^{C90S}-[^{15}N]UB^{K48R} oxyester indicate reduced intramolecular interaction between the L-side of Ube2r1C$^{C93S/YGY}$ and the hydrophobic patch of the donor ubiquitin. For Ube2g1 or Ube2r1C^{YGY} Lys-48-ubiquitylation activity, it is likely that the local structure formed by the acidic loop and the C-terminal region of the attached donor ubiquitin is more important than the simple positioning of the donor ubiquitin onto the L-side of the E2. These results suggest that Ube2g1, Ube2r1, and Ube2k, which are known to generate Lys-48-linked polyubiquitin efficiently without E3, seem to use a different mechanism to conjugate acceptor and donor ubiquitin. Other evidence supporting this idea is that the UB^{N60A} mutant displayed different Lys-48-ubiquitylation activities as an acceptor for Ube2k or Ube2g1, showing a severe defect with Ube2k, whereas ubiquitylation by Ube2g1 was relatively unaffected by the ubiquitin N60A mutation (12).

In the context of Ube2g1-UB oxyester, the acidic loop mutation (Y102G/Y104G) changes the chemical environment of the C-terminal region and the edge of the hydrophobic patch in the attached ubiquitin (Fig. 8*C* and Fig. 10*C*). The estimated K_m values of Ube2g1 and Ube2g1^{Y104G} showed that the acidic loop mutation also affected recruitment of the acceptor ubiquitin (Fig. 11). Moreover, production of a tiny amount of diubiquitin with linkage(s) other than to Lys-48 was identified with the E99G/D100G mutation (Fig. 12, see gel band indicated as *Di**); this suggests that the acidic loop also may play an important role in proper alignment of an acceptor ubiquitin. The production of non-Lys-48-linked diubiquitin was reported for Ube2d2 and Ube2b in the absence of E3 (8).

The acceptor ubiquitin can approach the active Cys residue via the R-side of Ube2g1∼UB thioester. Recently Ube2g2, a homolog of Ube2g1, was shown to form a functional dimer, and that residue Cys-48 residue is important for the dimerization (34). Because the Cys-48 residue is not conserved in Ube2g1 (Fig. 1) and Ube2g1 ubiquitylation activity is independent of the E2 concentration (Fig. 3), the mechanisms of ubiquitylation between Ube2g1 and Ube2g2 would be different from each other. The cognate E3 ligase(s) of Ube2g1 has not yet been identified; therefore, we have fit our model structure of the Ube2g1-UB oxyester (Fig. 10) to the Ube2g2·gp78-E3 complex structure reported by Das *et al.* (35). A fit was obtained without any steric clash and in which the R-side of Ube2g1, the candidate surface for an acceptor ubiquitin, is well exposed to solvent (not shown).

Interestingly, the recent docking model of Ube2r1∼UB thioester that was based on the Rosetta force field (and does not contain the acidic loop or the C-terminal extension) shows that the donor ubiquitin is located at the L-side region of Ube2r1, which is similar to our model for the Ube2g1^{C90S}-UB^{K48R} oxyester, where Ile-44 of the donor ubiquitin is close to Ser-129 of Ube2r1, and thus the I44A mutation of the donor ubiquitin can be suppressed by the S129L mutation of Ube2r1 (23). The introduction of two Tyr residues in the acidic loop of Ube2r1C reduced the interaction between the donor ubiquitin and the L-side of Ube2r1C^{YGY} but increased the Lys-48-ubiquitylation activity. The acidic loop of Ube2r1 displayed a lower binding affinity to the donor ubiquitin than did that of Ube2g1, and thus the acidic loop and the C-terminal tail of Ube2r1 might work together during the catalysis. It might be possible that the residues 184–196 of Ube2r1 stabilize the conformation of the donor ubiquitin in a manner similar to this Ube2r1∼UB thioester docking model (23) and thus facilitate the recruitment of an acceptor ubiquitin. Ube2r1 could adapt to its specific function in the presence of SCE-E3 by losing the ubiquitin binding property of its acidic loop.

Acidic loop or tail motifs are known to be important for the ubiquitylation activities of E2 or E3 enzymes; examples are the acidic loops in Ube2g1 and Ube2g2 (36), the acidic tail (residues 888–900) in human Nedd4 (HECT-E3) (37), and both acidic loop and acidic tail in Ube2r1 (10, 26, 38). These motifs possess both acidic and bulky hydrophobic residues and usually are near the active-site Cys residue. Although the acidic tail of Ube2r1 is far from the active site, it is known to interact with a donor ubiquitin of Ube2r1 (26, 39). Although the ubiquitin binding of the acidic tail of Nedd4 has not yet been identified, the others in Ube2g1 and Ube2r1 display a weak ubiquitin binding activity. HECT-E3 ligase could be similar with E2 enzyme, because the active Cys residue forms a labile thioester bond with a donor ubiquitin. We speculate that, as with the acidic loop of Ube2g1, the acidic tail of Nedd4 may interact with donor ubiquitin to enhance its ubiquitylation activity.

REFERENCES

1. Hershko, A., and Ciechanover, A. (1998) The ubiquitin system. *Annu. Rev. Biochem.* **67,** 425–479
2. Pickart, C. M. (2004) Back to the future with ubiquitin. *Cell* **116,** 181–190
3. Peng, J., Schwartz, D., Elias, J. E., Thoreen, C. C., Cheng, D., Marsischky, G., Roelofs, J., Finley, D., and Gygi, S. P. (2003) A proteomics approach to understanding protein ubiquitination. *Nat. Biotechnol.* **21,** 921–926
4. Houben, K., Dominguez, C., van Schaik, F. M., Timmers, H. T., Bonvin, A. M., and Boelens, R. (2004) Solution structure of the ubiquitin-conjugating enzyme UbcH5B. *J. Mol. Biol.* **344,** 513–526
5. VanDemark, A. P., Hofmann, R. M., Tsui, C., Pickart, C. M., and Wolberger, C. (2001) Molecular insights into polyubiquitin chain assembly: crystal structure of the Mms2/Ubc13 heterodimer. *Cell* **105,** 711–720
6. Eddins, M. J., Carlile, C. M., Gomez, K. M., Pickart, C. M., and Wolberger, C. (2006) Mms2-Ubc13 covalently bound to ubiquitin reveals the structural basis of linkage-specific polyubiquitin chain formation. *Nat. Struct.*

Mol. Biol. **13,** 915–920
7. Wickliffe, K. E., Lorenz, S., Wemmer, D. E., Kuriyan, J., and Rape, M. (2011) The mechanism of linkage-specific ubiquitin chain elongation by a single-subunit E2. *Cell* **144,** 769–781
8. Ryu, K. S., Choi, Y. S., Ko, J., Kim, S. O., Kim, H. J., Cheong, H. K., Jeon, Y. H., Choi, B. S., and Cheong, C. (2008) Direct characterization of E2-dependent target specificity and processivity using an artificial p27-linker-E2 ubiquitination system. *BMB Rep.* **41,** 852–857
9. Wu, K., Kovacev, J., and Pan, Z. Q. (2010) Priming and extending: a UbcH5/Cdc34 E2 handoff mechanism for polyubiquitination on a SCF substrate. *Mol. Cell* **37,** 784–796
10. Petroski, M. D., and Deshaies, R. J. (2005) Mechanism of lysine 48-linked ubiquitin-chain synthesis by the cullin-RING ubiquitin-ligase complex SCF-Cdc34. *Cell* **123,** 1107–1120
11. Haldeman, M. T., Xia, G., Kasperek, E. M., and Pickart, C. M. (1997) Structure and function of ubiquitin conjugating enzyme E2–25K: the tail is a core-dependent activity element. *Biochemistry* **36,** 10526–10537
12. Choi, Y. S., Jeon, Y. H., Ryu, K. S., and Cheong, C. (2009) 60th residues of ubiquitin and Nedd8 are located out of E2-binding surfaces, but are important for Lys-48 ubiquitin-linkage. *FEBS Lett.* **583,** 3323–3328
13. Shekhtman, A., Ghose, R., Goger, M., and Cowburn, D. (2002) NMR structure determination and investigation using a reduced proton (REDPRO) labeling strategy for proteins. *FEBS Lett.* **524,** 177–182
14. Fiaux, J., Bertelsen, E. B., Horwich, A. L., and Wüthrich, K. (2004) Uniform and residue-specific ^{15}N-labeling of proteins on a highly deuterated background. *J. Biomol. NMR* **29,** 289–297
15. Merkley, N., Barber, K. R., and Shaw, G. S. (2005) Ubiquitin manipulation by an E2 conjugating enzyme using a novel covalent intermediate. *J. Biol. Chem.* **280,** 31732–31738
16. Delaglio, F., Grzesiek, S., Vuister, G. W., Zhu, G., Pfeifer, J., and Bax, A. (1995) NMRPipe: a multidimensional spectral processing system based on UNIX pipes. *J. Biomol. NMR* **6,** 277–293
17. Goddard, T. D., and Kneller, D. G. SPARKY 3. University of California, San Francisco
18. Kiefer, F., Arnold, K., Künzli, M., Bordoli, L., and Schwede, T. (2009) The SWISS-MODEL repository and associated resources. *Nucleic Acids Res.* **37,** D387–D392
19. Shen, Y., Lange, O., Delaglio, F., Rossi, P., Aramini, J. M., Liu, G., Eletsky, A., Wu, Y., Singarapu, K. K., Lemak, A., Ignatchenko, A., Arrowsmith, C. H., Szyperski, T., Montelione, G. T., Baker, D., and Bax, A. (2008) Consistent blind protein structure generation from NMR chemical shift data. *Proc. Natl. Acad. Sci. U.S.A.* **105,** 4685–4690
20. Schneidman-Duhovny, D., Inbar, Y., Nussinov, R., and Wolfson, H. J. (2005) PatchDock and SymmDock: servers for rigid and symmetric docking. *Nucleic Acids Res.* **33,** W363–W367
21. Song, Y., DiMaio, F., Wang, R. Y., Kim, D., Miles, C., Brunette, T., Thompson, J., and Baker, D. (2013) High-resolution comparative modeling with RosettaCM. *Structure* **21,** 1735–1742
22. Hamilton, K. S., Ellison, M. J., Barber, K. R., Williams, R. S., Huzil, J. T., McKenna, S., Ptak, C., Glover, M., and Shaw, G. S. (2001) Structure of a conjugating enzyme-ubiquitin thiolester intermediate reveals a novel role for the ubiquitin tail. *Structure* **9,** 897–904
23. Saha, A., Lewis, S., Kleiger, G., Kuhlman, B., and Deshaies, R. J. (2011) Essential role for ubiquitin-ubiquitin-conjugating enzyme interaction in ubiquitin discharge from Cdc34 to substrate. *Mol. Cell* **42,** 75–83
24. Pettersen, E. F., Goddard, T. D., Huang, C. C., Couch, G. S., Greenblatt, D. M., Meng, E. C., and Ferrin, T. E. (2004) UCSF Chimera: a visualization system for exploratory research and analysis. *J. Comput. Chem.* **25,** 1605–1612
25. Gazdoiu, S., Yamoah, K., Wu, K., Escalante, C. R., Tappin, I., Bermudez, V., Aggarwal, A. K., Hurwitz, J., and Pan, Z. Q. (2005) Proximity-induced activation of human Cdc34 through heterologous dimerization. *Proc. Natl. Acad. Sci. U.S.A.* **102,** 15053–15058
26. Choi, Y. S., Wu, K., Jeong, K., Lee, D., Jeon, Y. H., Choi, B. S., Pan, Z. Q., Ryu, K. S., and Cheong, C. (2010) The human Cdc34 carboxyl terminus contains a non-covalent ubiquitin binding activity that contributes to SCF-dependent ubiquitination. *J. Biol. Chem.* **285,** 17754–17762
27. Ju, T., Bocik, W., Majumdar, A., and Tolman, J. R. (2010) Solution structure and dynamics of human ubiquitin conjugating enzyme Ube2g2. *Proteins* **78,** 1291–1301
28. Sakata, E., Satoh, T., Yamamoto, S., Yamaguchi, Y., Yagi-Utsumi, M., Kurimoto, E., Tanaka, K., Wakatsuki, S., and Kato, K. (2010) Crystal structure of UbcH5b approximately ubiquitin intermediate: insight into the formation of the self-assembled E2 approximately Ub conjugates. *Structure* **18,** 138–147
29. Kamadurai, H. B., Souphron, J., Scott, D. C., Duda, D. M., Miller, D. J., Stringer, D., Piper, R. C., and Schulman, B. A. (2009) Insights into ubiquitin transfer cascades from a structure of a UbcH5B approximately ubiquitin-HECT(NEDD4L) complex. *Mol. Cell* **36,** 1095–1102
30. Pruneda, J. N., Stoll, K. E., Bolton, L. J., Brzovic, P. S., and Klevit, R. E. (2011) Ubiquitin in motion: structural studies of the ubiquitin-conjugating enzyme approximately ubiquitin conjugate. *Biochemistry* **50,** 1624–1633
31. Brzovic, P. S., Lissounov, A., Christensen, D. E., Hoyt, D. W., and Klevit, R. E. (2006) A UbcH5/ubiquitin noncovalent complex is required for processive BRCA1-directed ubiquitination. *Mol. Cell* **21,** 873–880
32. Wu, P. Y., Hanlon, M., Eddins, M., Tsui, C., Rogers, R. S., Jensen, J. P., Matunis, M. J., Weissman, A. M., Weisman, A. M., Weissman, A. M., Wolberger, C., Wolberger, C. P., and Pickart, C. M. (2003) A conserved catalytic residue in the ubiquitin-conjugating enzyme family. *EMBO J.* **22,** 5241–5250
33. Pruneda, J. N., Littlefield, P. J., Soss, S. E., Nordquist, K. A., Chazin, W. J., Brzovic, P. S., and Klevit, R. E. (2012) Structure of an E3:E2~Ub complex reveals an allosteric mechanism shared among RING/U-box ligases. *Mol. Cell* **47,** 933–942
34. Liu, W., Shang, Y., Zeng, Y., Liu, C., Li, Y., Zhai, L., Wang, P., Lou, J., Xu, P., Ye, Y., and Li, W. (2014) Dimeric Ube2g2 simultaneously engages donor and acceptor ubiquitins to form Lys48-linked ubiquitin chains. *EMBO J.* **33,** 46–61
35. Das, R., Liang, Y. H., Mariano, J., Li, J., Huang, T., King, A., Tarasov, S. G., Weissman, A. M., Ji, X., and Byrd, R. A. (2013) Allosteric regulation of E2:E3 interactions promote a processive ubiquitination machine. *EMBO J.* **32,** 2504–2516
36. Li, W., Tu, D., Brunger, A. T., and Ye, Y. (2007) A ubiquitin ligase transfers preformed polyubiquitin chains from a conjugating enzyme to a substrate. *Nature* **446,** 333–337
37. Maspero, E., Valentini, E., Mari, S., Cecatiello, V., Soffientini, P., Pasqualato, S., and Polo, S. (2013) Structure of a ubiquitin-loaded HECT ligase reveals the molecular basis for catalytic priming. *Nat. Struct. Mol. Biol.* **20,** 696–701
38. Kleiger, G., Saha, A., Lewis, S., Kuhlman, B., and Deshaies, R. J. (2009) Rapid E2-E3 assembly and disassembly enable processive ubiquitylation of cullin-RING ubiquitin ligase substrates. *Cell* **139,** 957–968
39. Spratt, D. E., and Shaw, G. S. (2011) Association of the disordered C-terminus of CDC34 with a catalytically bound ubiquitin. *J. Mol. Biol.* **407,** 425–438